Asian Journal of Andrology (2021) 23, 627–632
www.asiaandro.com; www.ajandrology.com

Open Access

ORIGINAL ARTICLE

Sperm Biology

Novel biallelic loss-of-function mutations in *CFAP43* cause multiple morphological abnormalities of the sperm flagellum in Pakistani families

Ihsan Khan*, Basit Shah*, Sobia Dil, Nadeem Ullah, Jian-Teng Zhou, Da-Ren Zhao, Yuan-Wei Zhang, Xiao-Hua Jiang, Ranjha Khan, Asad Khan, Haider Ali, Muhammad Zubair, Wasim Shah, Huan Zhang, Qing-Hua Shi

Multiple morphological abnormalities of the sperm flagella (MMAF) is a specific type of asthenoteratozoospermia, presenting with multiple morphological anomalies in spermatozoa, such as absent, bent, coiled, short, or irregular caliber flagella. Previous genetic studies revealed pathogenic mutations in genes encoding cilia and flagella-associated proteins (*CFAPs*; *e.g.*, *CFAP43*, *CFAP44*, *CFAP65*, *CFAP69*, *CFAP70*, and *CFAP251*) responsible for the MMAF phenotype in infertile men from different ethnic groups. However, none of them have been identified in infertile Pakistani males with MMAF. In the current study, two Pakistani families with MMAF patients were recruited. Whole-exome sequencing (WES) of patients and their parents was performed. WES analysis reflected novel biallelic loss-of-function mutations in *CFAP43* in both families (Family 1: ENST00000357060.3, p.Arg300Lysfs*22 and p.Thr526Serfs*43 in a compound heterozygous state; Family 2: ENST00000357060.3, p.Thr526Serfs*43 in a homozygous state). Sanger sequencing further confirmed that these mutations were segregated recessively in the families with the MMAF phenotype. Semiquantitative reverse-transcriptase polymerase chain reaction (qRT-PCR) was carried out to detect the effect of the mutation on mRNA of the affected gene. Previous research demonstrated that biallelic loss-of-function mutations in *CFAP43* accounted for the majority of all *CFAP43*-mutant MMAF patients. To the best of our knowledge, this is the first study to report *CFAP43* biallelic loss-of-function mutations in a Pakistani population with the MMAF phenotype. This study will help researchers and clinicians to understand the genetic etiology of MMAF better.

Asian Journal of Andrology (2021) **23**, 627–632; doi: 10.4103/aja.aja_26_21; published online: 28 May 2021

Keywords: cilia and flagella-associated proteins; male infertility; multiple morphological abnormalities of the sperm flagella; whole-exome sequencing

INTRODUCTION

Multiple morphological abnormalities of the sperm flagellum (MMAF) is one of the more severe forms of sperm defect,[1] characterized by bent, coiled, irregular, short, or absent sperm flagella.[2–6] The sperm flagellum in MMAF patients often shows ultrastructural abnormalities associated with the "9 + 0" arrangement of dynein microtubules, such as lacking the central pair of microtubules, disorganized axoneme, and mitochondrial sheath, which in turn affects sperm motility and leads to male infertility.[4,7–9]

In the past few years, the development of next-generation sequencing technology has led to identification of a genetic cause in MMAF patients. Various pathogenic mutations have been found in genes encoding cilia and flagella-associated proteins (*CFAPs*), such as *CFAP43*, *CFAP44*, *CFAP65*, *CFAP69*, *CFAP70*, and *CFAP251*.[2,5,10–19] It has been noted that all these *CFAP*-associated genes have diverse functions and location. For example, *CFAP43*, *CFAP44,* and *CFAP65* are associated with the inner dynein arm (IDA) complex tether/tether head (T/TH); *CFAP69* is associated with intraflagellar transport (IFT); *CFAP70* is related to the outer dynein arm (ODA)-associated complex; and *CFAP251* is identified in the calmodulin and spoke-associated complex (CSC).[1] In 2017, Tang *et al.*[2] identified biallelic loss-of-function mutations of *CFAP43* in Chinese MMAF patients and further confirmed the pathogenicity in knockout mouse models of the *Cfap43* ortholog gene. Later, in 2018, Coutton *et al.*[10] also identified *CFAP43* biallelic mutations in MMAF patients from different ethnic groups. Biallelic mutations of *CFAP43* and *CFAP44* have been reported to be account for approximately 8%–31% of studied MMAF cohorts.[2,10,11] However, the genetic causes of MMAF among Pakistani patients remain unexplored. Given the existence of a traditional and close-knit society in Pakistan, approximately 65% of the population have consanguineous marriages.[20] A high proportion of consanguineous marriage increases the risk of autosomal recessive disorders in offspring. Such kinds of

First Affiliated Hospital of USTC, Hefei National Laboratory for Physical Sciences at Microscale, the CAS Key Laboratory of Innate Immunity and Chronic Disease, School of Basic Medical Sciences, Division of Life Sciences and Medicine, CAS Center for Excellence in Molecular Cell Science, Collaborative Innovation Center of Genetics and Development, University of Science and Technology of China, Hefei 230027, China.
*These authors contributed equally to this work.
Correspondence: Dr. QH Shi (qshi@ustc.edu.cn) or Dr. H Zhang (zhh1985@ustc.edu.cn)
Received: 21 September 2020; Accepted: 07 February 2021

autosomal recessive disease with identified genetic causes have been reported in the Pakistani population including primary microcephaly,[21] deafness,[22] retinitis pigmentosa,[23] and infertility.[24,25] Therefore, we wondered, whether *CFAP43* mutations could be one of the genetic causes for Pakistani MMAF patients.

CFAP43 (also known as WDR96, ENST00000357060.3) is localized on chromosome 10 and contains 38 exons encoding a predicted 1665-amino-acid protein (Q8NDM7), specifically expressed in the human testis,[11] and plays a vital role in the organization of the sperm flagellar axoneme. Animal model studies (knock out of *CFAP43* and *CFAP44* homologs in mice and *Trypanosoma brucei*) have produced evidence that mutations in these genes destabilize the entire complex, leading to both periaxonemal and axonemal defects and resulting in aborted flagella.[10] However, owing to the absence of a specific antibody for *CFAP43*, the specific role and localization of the CFAP43 protein in the mouse testis and their molecular and cellular mechanisms are yet to be elucidated.[26]

We recruited two Pakistani families with three infertile men suffering from MMAF. Through whole-exome sequencing (WES) and Sanger sequencing, we identified novel biallelic loss-of-function mutations in *CFAP43* in both families (Family 1: ENST00000357060.3, c.899_900del and c.1577_1578del in a compound heterozygous state; Family 2: ENST00000357060.3, c.1577_1578del in a homozygous state). Mutation (c.1577_1578del) was identified in both families and caused mRNA degradation in spermatozoa of the Family 2 patient.

To our knowledge, this is the first report that *CFAP43* biallelic loss-of-function mutations cause MMAF in Pakistani populations. This study will help researchers and clinicians to better understand the genetic etiology of MMAF and would be of high interest for genetic counseling and diagnosis of MMAF.

PARTICIPANTS AND METHODS

Study participants

Two Pakistani families with three interfile men were recruited. Written informed consent was obtained from all the affected and control family members. This study was approved by the Institutional Ethical Committee of University of Science and Technology of China (USTC; Hefei, China) with the approval number of USTCEC202000003.

Semen analysis

All three patients had routine semen analysis performed twice according to the World Health Organization guidelines (2010).[27] Sperm morphology was assessed as previously described by Zhang *et al.*[24] The fixed smear slides were sequentially immersed for 30 s in ethanol of 80% and 50% concentration and washed with purified water and then placed in hematoxylin stain (Solarbio, Beijing, China) for 4 min followed by serially immersed for 30 s in purified water, acidic ethanol, running cold tap water, and ethanol of 50%, 80%, and 95% concentration, respectively. These slides were then dipped in Orange-G-6 stain (Solarbio) for 1 min and washed three times with 95% of ethanol. Finally, the slides were forward to Eosin Azure Stain (Solarbio) for 1 min and then washed with 95% and 100% ethanol in each two times for 30 s. These slides were then dipped in xylene:ethanol (1:1 ratio) for 1 min in a fume hood. At least 200 stained spermatozoa per sample were examined by optical microscopy (Nikon Eclipse 80i, Nikon, Tokyo, Japan). According to their characteristic defects, the morphological abnormalities of sperm flagella were divided into five categories: short, coiled, absent, bent, and irregular/caliber.

WES, sequencing data analysis, and Sanger sequencing

Genomic DNA was extracted from the peripheral blood of all available family members by using FlexiGene DNA Kit (QIAGEN, Hilden, Germany) as per the manufacturer's instructions. For WES, AIExome Enrichment Kit V1 (iGeneTech, Beijing, China)-captured libraries were constructed for family members of Family 1 (I:1, I:2, II:1, and II:2) and Family 2 (III:1, III:2, IV:3, and IV:4) as instructed by the manufacturer. Sequencing was carried out on a Hiseq2000 platform (Illumina, San Diego, CA, USA). Clean reads were mapped to the human reference genome (hg19) by Burrows–Wheeler Alignment tool.[28] Variants were discovered and annotated by the Genome Analysis Toolkit (GATK)[29] and ANNOVAR.[30] After that, specific filtration pipelines for each family are described in **Supplementary Figure 1** and detailed in **Supplementary Table 2** and **Supplementary Table 3**. Sanger sequencing was performed to verify the selected variants in all the available family members. The primers for PCR are listed in **Supplementary Table 1**.

Transmission electron microscopic (TEM) analysis of spermatozoa

TEM analysis was performed according to Zhang *et al.*[31] in 2019. Spermatozoa from the patient and a fertile control individual were taken and fixed in 0.1 mol l^{-1} phosphate buffer (PB; pH 7.4), comprising 0.2% picric acid, 8% glutaraldehyde, and 4% paraformaldehyde and stored at 4°C overnight. Samples were washed with 0.1 mol l^{-1} PB, postfixed with 1% osmium tetroxide. Spermatozoa cells were dehydrated through graded alcohol (30%, 60%, 90%, 100%, 100%, and 100%; 10 min for each bath) followed by infiltration of an epon resin and acetone mixture. Ultrathin (70 nm) sections were cut from the samples followed by staining with lead citrate and uranyl acetate. Tecnai 10 or 12 Microscopes (Philips CM10, Philips Electronics, Eindhoven, The Netherlands) at 120 kV or 100 kV were used to capture and examine the ultrastructure of the samples.

RNA extraction and semiquantitative reverse-transcriptase polymerase chain reaction (qRT-PCR)

Total sperm RNA from patient (Family 2-IV:3) and a fertile male was extracted with RNAiso Plus (TAKARA, Beijing, China) and reverse-transcribed into cDNA by PrimeScript RT Reagent Kit (TAKARA) as per the manufacturer's instructions. Glyceraldehyde-3-phosphate dehydrogenase (GAPDH) (forward: 5'-GTCAAGGCTGAGAACGGGAA-3'; reverse: 5'-AAATGAGCCCCAGCCTTCTC-3') was used as an internal control and *CFAP43* (Ensembl transcript ID: ENST00000357060.3) primers used were as follows, forward: 5'-AGCACGTCGTTTATGATCAG-3'; reverse: 5'-TGTGGCAGTAATGTAGGCAG-3'.

RESULTS

Clinical features of patients

This study was performed on two Pakistani families with three infertile men. Family 1-II:1 (57 years), Family 1-II:2 (55 years), and Family 2-IV:3 (39 years) had been married for 31 years, 26 years, and 14 years, respectively, but all were infertile. Detailed information was collected from each patient to exclude the possibility of associated infertility-related disease. All the individuals were healthy, with no previous history of any testicular injury or obstruction, no symptoms of Primary Ciliary Dyskinesia (PCD; disease ID: #MIM 244400). Detailed pedigree charts were constructed on the basis of information provided by their parents (**Figure 1**). All the physical characteristics and semen parameter values of the patients are presented in **Table 1**. The semen volumes, pH, and viscosity fell within the normal ranges according to the World Health Organization guidelines (2010).[27] However, sperm concentrations were lower than the normal range (**Table 1**). Sperm morphological analysis reflected severe abnormalities of flagella including bent, short, coiled, irregular, and absent that are typical characteristics of MMAF (**Figure 2a**).

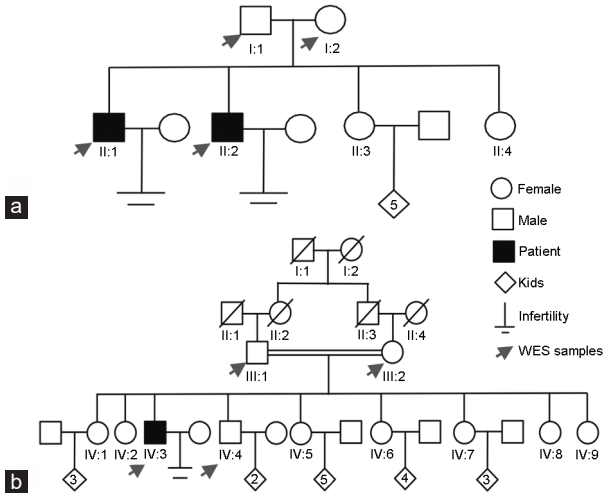

Figure 1: Pedigree of (**a**) Family 1 and (**b**) Family 2. Two Pakistani families with three infertile patients were recruited. I, II, III, and IV represent generation 1, 2, 3, and 4, respectively. Squares represent males, circles represent females, diamonds indicate offspring, and the inside numerals indicate the number of offspring. The slashes denote deceased family members. Solid squares indicate patients. Parallel slash lines indicate consanguineous marriage. Red arrows indicate the members selected for WES. WES: whole-exome sequencing.

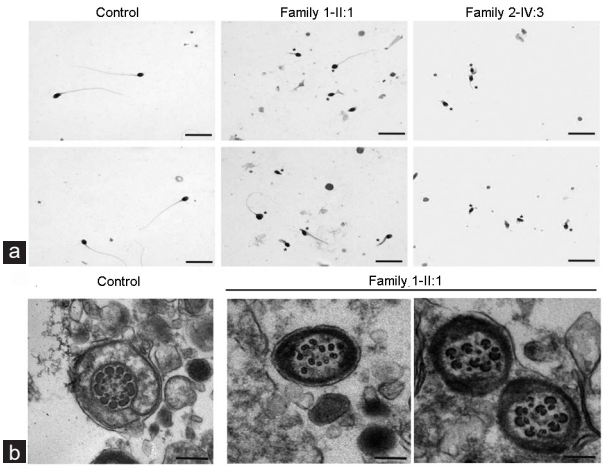

Figure 2: Morphology and transmission electron microscopic analysis of spermatozoa from normal control and infertile patients. (**a**) Most spermatozoa of patients (middle and right panels) presented abnormal sperm flagella (*), compared with control spermatozoa (left panel). Scale bars = 10 μm. (**b**) Cross-section of fertile male spermatozoa (left panel). An axoneme of a fertile male's spermatozoa comprised DMTs circularly arranged around a CPC of microtubules (9 + 2 organization), surrounded by ODFs and FS. Cross-section of the patient II:1 of Family 1 (*CFAP43*-deficient), see right panel. Spermatozoa display totally disorganized axoneme; outer dense fibers and peripheral microtubules are misarranged. The central pair is displaced. Scale bars = 500 nm. DMTs: doublets of microtubules; CPC: central pair complex; ODF: outer dense fiber; FS: fibrous sheath; CFAP: cilia and flagella-associated protein.

Novel biallelic loss-of-function mutations in CFAP43 are candidate pathogenic variants in the families

To identify the genetic cause of MMAF, WES was performed for all available family members as shown in **Figure 1**. WES data were filtered according to the detailed pipeline in **Supplementary Figure 1**. As stated in a previous study, MMAF is an autosomal recessive inheritance,[17] so as from the family history of Family 1, and the parents in Family 2 were in a consanguineous marriage, we focused on homozygous/compound heterozygous mutations shared by patients. Finally, the filtration pipeline identified novel biallelic loss-of-function mutations in *CFAP43* in both families (Family 1: ENST00000357060.3, c.899_900del and c.1577_1578del in a compound heterozygous state; Family 2: ENST00000357060.3, c.1577_1578del in a homozygous state). It is noteworthy that the frameshift mutation (c.1577_1578del) was identified in both families.

CFAP43 mutation induced severe axonemal disorganization

TEM was performed to observe the ultrastructure defects of patient II:1's spermatozoa of Family 1, as well as normal sperm ultrastructure from a fertile control individual. For TEM, a typical microtubule structure was presented in the spermatozoa of the fertile control that contains a "9 + 2" axonemal arrangement of nine doublets of microtubules (DMTs) and two central pairs (CP), surrounded by a fibrous sheath (FS) and outer dense fibers (ODF) as shown in **Figure 2b**. In contrast to the fertile male spermatozoa, *CFAP43*-defecient sperm cross-sections showed axonemal and periaxonemal defects and approximately 82% of the cross-sections were abnormal (**Figure 2b**). The main defect was severe disorganization of the FS, ODF, and axonemal disassembly, and in some cross-sections the absence of central pair complex (CPC) (9 + 0 conformation).

CFAP43 mutations cosegregated with MMAF phenotype in the families and induced CFAP43 mRNA decay

Sanger sequencing confirmed that the WES-identified *CFAP43* mutations cosegregated with MMAF phenotype in both families (**Figure 3a** and **3b**). To determine the effects of the frameshift mutation (c.1577_1578del) on CFAP43 expression, we measured *CFAP43* mRNA in spermatozoa of the patient from Family 2, using the sperm sample from a fertile male as control. As shown in **Figure 3c**, *CFAP43* mRNA was detected in the control sample, but not in the patient IV:3. Owing to the unavailability of Family 1 patients' fresh semen samples for mutant *CFAP43* protein/mRNA detection, we compared the mutation c.899_900del with reported *CFAP43* mutations that had been confirmed in mRNA or protein level. Our mutation, c.899_900del (predicted truncate protein, p.Arg300Lysfs*22), was close to p.Asn380Lysfs*3, which was previously identified by Wu *et al.*[11] and has been confirmed to cause mRNA decay by quantitative polymerase chain reaction (qPCR), as well as the lack of CFAP43 protein by immunofluorescent staining in patients' semen samples.

DISCUSSION

In the current study, we recruited two Pakistani families with MMAF patients. After WES of all available family members, novel biallelic loss-of-function mutations in *CFAP43* were identified in both families (Family 1: ENST00000357060.3, c.899_900del and c.1577_1578del in a compound heterozygous state; Family 2: ENST00000357060.3, c.1577_1578del in a homozygous state), as shown in **Figure 4**. Sanger sequencing further confirmed that these mutations were segregated recessively in the families with MMAF phenotype. Furthermore, the mutation c.1577_1578del has been confirmed to cause mRNA degradation in patient's spermatozoa from the Family 2. TEM results of the patient II:1's spermatozoa of Family 1 showed severe disorganization of the axoneme. This is the first report of novel biallelic loss-of-function mutations in *CFAP43* causing MMAF in the Pakistani population.

Of all identified *CFAP43* mutations, 80% are loss-of-function mutations, which include frameshift, nonsense, and splice-site mutations (**Figure 5** and **Supplementary Table 4**[Ref 2,10,11,32]). These loss-of-function mutations (frameshift and nonsense) might cause

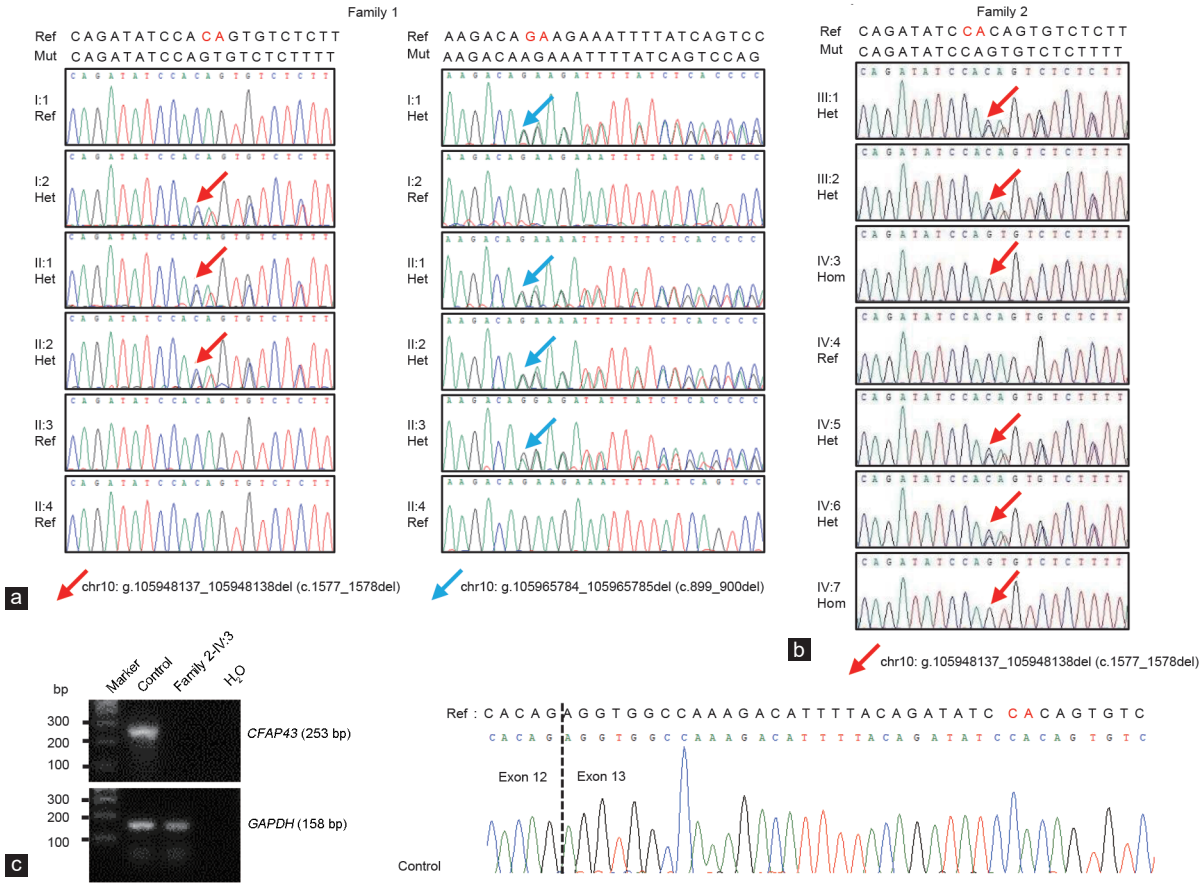

Figure 3: Sanger sequencing results of *CFAP43* mutations in DNA and mRNA levels. Chromatograms of the *CFAP43* mutations from (**a**) Family 1 and (**b**) Family 2. Red/Blue arrows show the genomic position of *CFAP43* mutations. (**c**) SqRT-PCR analysis of *CFAP43* mRNA levels in male control and Family 2-IV:3 sperm samples. SqRT-PCR: semiquantitative reverse-transcriptase polymerase chain reaction; *CFAP*: cilia and flagella-associated protein; bp: base pair; Ref: reference; Het: heterozygous; chr10: chromosome 10; *GAPDH*: glyceraldehyde-3-phosphate dehydrogenase; del: deletion.

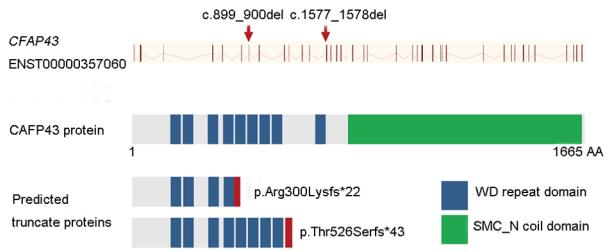

Figure 4: The identified mutations in *CFAP43* gene and predicted mutant proteins. *CFAP43* gene structure (Ensembl transcript ID: ENST00000357060) is shown with mutations identified in both families. Vertical bars indicate exons and slashed lines represent introns. CFAP43 (1665 AA) comprises two domains: WD (tryptophan-aspartic acid (W-D)) repeat domain and SMC_N coil domain. *CFAP*: cilia and flagella-associated protein; AA: amino acid; SMC_N: N-terminus of structural maintenance of chromosome; del: deletion.

mRNA degradation or produce truncate protein. Detailed sperm analyses indicated an increased number of immotile spermatozoa (98%–100%), and all patients' spermatozoa had typical MMAF characteristics. Furthermore, no significant differences were observed among the semen parameters of the patients harboring *CFAP43* mutations in the current study compared with the previously reported patients with other *CFAP43* mutations (**Supplementary Table 4**). Wu *et al.*[11] first examined two *CFAP43* mutations' effects (p.Asn380Lysfs*3 and p.Gln492Arg) on mRNA and protein level in patients' spermatozoa and found that both mutations cause *CFAP43* mRNA degradation. In the current study, we could not obtain fresh semen samples from patients of Family 1 to verify the *CFAP43* mutation effects on mRNA and protein level. However, since the mutation (p.Arg300Lysfs*22) is close to the mutations verified by Wu *et al.*[11] (p.Asn380Lysfs*3 and p.Gln492Arg), we speculate that *CFAP43* mutations identified in our study have a similar effect on *CFAP43* expression, resulting in complete loss of *CFAP43* (**Figure 4**).

CFAP43 and *CFAP44* mutations account for 7.5%–30.8% of MMAF patients from a different study cohort, specified in a recent review.[1] Tang *et al.*[2] identified patients harboring *CFAP44* or *CFAP43* mutations, explaining 7.5% (4/30) of all patients with MMAF. However, Yan *et al.*[32] identified 22.2% of 27 patients carrying *CFAP44* or *CFAP43* mutations. The most recent study by Wu *et al.*[11] reported 30.8% of all patients **Supplementary Table 5**[Ref 2,7,11,12,15,18,32–35] summarized the percentages of involvement of *CFAP43* and *CFAP44*, as well as other MMAF reported genes in different cohorts. Until now, only *CFAP43* mutations have been identified in Pakistani MMAF patients in the current study.

According to previous information, good intracytoplasmic sperm injection (ICSI) outcomes are reported for MMAF patients with *CFAP43* and *CFAP44* mutations. The recorded rates of transferable embryo, implantation, and clinical pregnancy were 80%, 50%, and 100%, respectively, in *CFAP43*.[5] Hence, it is worth mentioning that it would be more interesting for researchers and clinicians to apply ICSI for *CFAP43*-mutant MMAF patients and

Table 1: Characteristics and sperm morphology in the patients

Characteristic	*Reference value*[a]	*Family 1–II:1*	*Family 1–II:2*	*Family 2–IV:3*
Genotype	–	c.899_900del/ c.1577_1578del	c.899_900del/ c.1577_1578del	c.1577_1578del/ c.1577_1578del
Age (year)[b]	–	57	55	39
Years of marriage[c]	–	31	26	14
BMI (kg m^{-2})	–	37.1	31.3	23.5
Semen parameters				
Semen volume (ml)	>1.5	2.0	3.0	3.3
Semen pH	Alkaline	Alkaline	Alkaline	Alkaline
Sperm concentration (× 10^6 ml^{-1})	>15	9	6	7
Motility (%)	>40	0	0	0
Progressively motility (%)	>32	0	0	0
Sperm morphology				
Normal flagella (%)	>4.0	3.2	–	0.8
Abnormal flagella (%)	–	96.7	–	99.1
Short flagella (%)	–	70.9	–	44.5
Absent flagella (%)	–	17.2	–	18.3
Bent flagella (%)	–	5.4	–	14.9
Coiled flagella (%)	–	5.0	–	12.6
Irregular/caliber (%)	–	0	–	8.8
Head defects				
Normal head (%)	–	6.8	–	4.9
Abnormal head (%)	–	93.1	–	95.2
Tapered head (%)	–	45.9	–	71.1
Pyriform head (%)	–	25.0	–	14.7
Double head (%)	–	1.4	–	0.9
Large/amorphous head (%)	–	0	–	0.9
Round head (%)	–	10.9	–	5.5
Small head (%)	–	6.5	–	0.9
Absent head (%)	–	3.4	–	1.2

[a]Reference values were published in WHO (2010). [b]The current ages. [c]The current years of marriage. –: not available; BMI: body mass index; WHO: World Health Organization; del: deletion

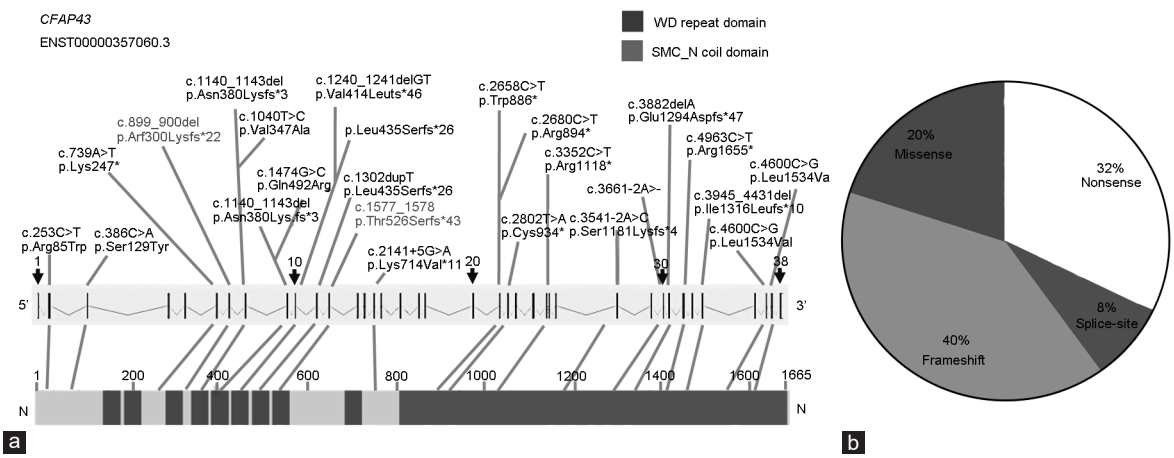

Figure 5: Summary of all reported *CFAP43* mutations in MMAF patients. (**a**) All compound heterozygous mutations are listed above the gene map; horizontal connections represent two mutations identified in one patient. All homozygous mutations are listed below the gene map. Red ones indicate the mutations identified in current study. (**b**) Statistic of all *CFAP43* mutations. *CFAP*: cilia and flagella-associated protein; MMAF: multiple morphological abnormalities of the sperm flagella; del: deletion; WD: tryptophan-aspartic acid (W-D).

improving the prediction of ICSI outcomes for MMAF patients in Pakistan. However, it is very important to know the genetic screening of the wives of male patients carrying *CFAP43* mutation before the couple asks for ICSI, to reduce the chances of genetic diseases in the offspring.

In conclusion, our study identified novel loss-of-function mutations in *CFAP43* in Pakistani MMAF patients. These findings highlight the significance for genetic counseling and diagnosis for MMAF patients in the Pakistani population, while *CFAP43* could be routinely genetic diagnosed. Further studies are needed to identify

other pathogenic genes to characterize better MMAF in the Pakistani population.

AUTHOR CONTRIBUTIONS

IK and BS wrote the manuscript and performed semen analysis; SD, NU, AK, HA, XHJ, WS, MZ, and RK collected patients' samples. JTZ, DRZ, and YWZ performed the WES sequencing and WES data analysis. QHS and HZ conceived and supervised the study, designed and analyzed data, and wrote the manuscript. All authors read and approved the final manuscript.

COMPETING INTERESTS

All authors declared no competing interests.

ACKNOWLEDGMENTS

This work was supported by the National Natural Science Foundation of China (No. 32070850), the National Natural Science Foundation of China (No. 31630050, 31890780, and 32061143006), the National Key Research and Developmental Program of China (2018YFC1003900, 2019YFA0802600, and 2016YFC1000600), the Strategic Priority Research Program of the Chinese Academy of Sciences (No. XDB19000000), and the Fundamental Research Funds for the Central Universities (No. YD2070002006).

Supplementary Information is linked to the online version of the paper on the *Asian Journal of Andrology* website.

REFERENCES

1 Touré A, Martinez G, Kherraf ZE, Cazin C, Beurois J, *et al*. The genetic architecture of morphological abnormalities of the sperm tail. *Hum Genet* 2021; 140: 21–42.
2 Tang S, Wang X, Li W, Yang X, Li Z, *et al*. Biallelic mutations in *CFAP43* and *CFAP44* cause male infertility with multiple morphological abnormalities of the sperm flagella. *Am J Hum Genet* 2017; 100: 854–64.
3 Chemes HE, Brugo S, Zanchetti F, Carrere C, Lavieri JC. Dysplasia of the fibrous sheath: an ultrastructural defect of human spermatozoa associated with sperm immotility and primary sterility. *Fertil Steril* 1987; 48: 664–9.
4 Rawe V, Galaverna G, Acosta A, Olmedo SB, Chemes H. Incidence of tail structure distortions associated with dysplasia of the fibrous sheath in human spermatozoa. *Hum Reprod* 2001; 16: 879–86.
5 Sha YW, Wang X, Su ZY, Mei LB, Ji ZY, *et al*. Patients with multiple morphological abnormalities of the sperm flagella harbouring *CFAP44* or *CFAP43* mutations have a good pregnancy outcome following intracytoplasmic sperm injection. *Andrologia* 2019; 51: 131–51.
6 Barthelemy C, Tharanne M, Lebos C, Lecomte P, Lansac J. Tail stump spermatozoa: morphogenesis of the defect. An ultrastructural study of sperm and testicular biopsy. *Andrologia* 1990; 22: 417–25.
7 Khelifa MB, Coutton C, Zouari R, Karaouzène T, Rendu J, *et al*. Mutations in *DNAH1*, which encodes an inner arm heavy chain dynein, lead to male infertility from multiple morphological abnormalities of the sperm flagella. *Am J Hum Genet* 2014; 94: 95–104.
8 Yang SM, Li HB, Wang JX, Shi YC, Cheng HB, *et al*. Morphological characteristics and initial genetic study of multiple morphological anomalies of the flagella in China. *Asian J Androl* 2015; 17: 513.
9 Chemes HE, Rawe VY. Sperm pathology: a step beyond descriptive morphology. Origin, characterization and fertility potential of abnormal sperm phenotypes in infertile men. *Hum Reprod Update* 2003; 9: 405–28.
10 Coutton C, Vargas AS, Amiri-Yekta A, Kherraf ZE, Mustapha SF, *et al*. Mutations in CFAP43 and CFAP44 cause male infertility and flagellum defects in *Trypanosoma* and human. *Nat Commun* 2018; 9: 1–18.
11 Wu H, Li W, He X, Liu C, Fang Y, *et al*. Novel *CFAP43* and *CFAP44* mutations cause male infertility with multiple morphological abnormalities of the sperm flagella (MMAF). *Reprod Biomed Online* 2019; 38: 769–78.
12 Wang WL, Tu CF, Nie HC, Meng LL, Li Y, *et al*. Biallelic mutations in *CFAP65* lead to severe asthenoteratospermia due to acrosome hypoplasia and flagellum malformations. *J Med Genet* 2019; 56: 750–7.
13 Liu CY, Lv MR, He XJ, Zhu Y, Amiri-Yekta A, *et al*. Homozygous mutations in *SPEF2* induce multiple morphological abnormalities of the sperm flagella and male infertility. *J Med Genet* 2020; 57: 31–7.
14 Liu CY, He XJ, Liu WJ, Yang SM, Wang LB, *et al*. Bi-allelic mutations in *TTC29* cause male subfertility with asthenoteratospermia in humans and mice. *Am J Hum Genet* 2019; 105: 1168–81.
15 Kherraf ZE, Amiri-Yekta A, Dacheux D, Karaouzene T, Coutton C, *et al*. A homozygous ancestral SVA-insertion-mediated deletion in *WDR66* induces multiple morphological abnormalities of the sperm flagellum and male infertility. *Am J Hum Genet* 2018; 103: 400–12.
16 Auguste Y, Delague V, Desvignes JP, Longepied G, Gnisci A, *et al*. Loss of calmodulin- and radial-spoke-associated complex protein CFAP251 leads to immotile spermatozoa lacking mitochondria and infertility in men. *Am J Hum Genet* 2018; 103: 413–20.
17 He XJ, Li WY, Wu H, Lv MR, Liu WJ, *et al*. Novel homozygous *CFAP69* mutations in humans and mice cause severe asthenoteratospermia with multiple morphological abnormalities of the sperm flagella. *J Med Genet* 2019; 56: 96–103.
18 Dong FN, Amiri-Yekta A, Martinez G, Saut A, Tek J, *et al*. Absence of *CFAP69* causes male infertility due to multiple morphological abnormalities of the flagella in human and mouse. *Am J Hum Genet* 2018; 102: 636–48.
19 Beurois J, Martinez G, Cazin C, Kherraf ZE, Amiri-Yekta A, *et al*. *CFAP70* mutations lead to male infertility due to severe astheno-teratozoospermia. A case report. *Hum Reprod* 2019; 34: 2071–9.
20 Manzoor R, Imran W, Maken A, Syed T. Consanguineous marriages: effects on pregnancy outcomes in Pakistan. *J Dev Policy Pract* 2018; 2: 78–105.
21 Ansar M, Ebstein F, Özkoç H, Paracha SA, Iwaszkiewicz J, *et al*. Biallelic variants in *PSMB1* encoding the proteasome subunit β6 cause impairment of proteasome function, microcephaly, intellectual disability, developmental delay and short stature. *Hum Mol Genet* 2020; 29: 1132–43.
22 Santos-Cortez RL, Faridi R, Rehman AU, Lee K, Ansar M, *et al*. Autosomal-recessive hearing impairment due to rare missense variants within *S1PR2*. *Am J Hum Genet* 2016; 98: 331–8.
23 Khan MI, Kersten FF, Azam M, Collin RW, Hussain A, *et al*. *CLRN1* mutations cause nonsyndromic retinitis pigmentosa. *Ophthalmology* 2011; 118: 1444–8.
24 Zhang B, Ma H, Khan T, Ma A, Li T, *et al*. A *DNAH17* missense variant causes flagella destabilization and asthenozoospermia. *J Exp Med* 2020; 217: e20182365.
25 Yin H, Ma H, Hussain S, Zhang H, Xie X, *et al*. A homozygous *FANCM* frameshift pathogenic variant causes male infertility. *Genet Med* 2018; 21: 62–70.
26 Yu Y, Wang J, Zhou L, Li H, Zheng B, *et al*. *CFAP43*-mediated intra-manchette transport is required for sperm head shaping and flagella formation. *Zygote* 2021; 29: 75–81.
27 World Health Organization. Laboratory Manual for the Examination and Processing of Human Semen. 5th ed. Geneva: WHO Press; 2010.
28 Li H, Durbin R. Fast and accurate short read alignment with Burrows–Wheeler transform. *Bioinformatics* 2009; 25: 1754–60.
29 McKenna A, Hanna M, Banks E, Sivachenko A, Cibulskis K, *et al*. The Genome Analysis Toolkit: a MapReduce framework for analyzing next-generation DNA sequencing data. *Genome Res* 2010; 20: 1297–303.
30 Wang K, Li MY, Hakonarson H. ANNOVAR: functional annotation of genetic variants from high-throughput sequencing data. *Nucleic Acids Res* 2010; 38: e164.
31 Zhang B, Khan I, Liu C, Ma A, Khan A, *et al*. Novel loss-of-function variants in *DNAH17* cause multiple morphological abnormalities of the sperm flagella in humans and mice. *Clin Genet* 2020; 99: 176–86.
32 Sha YW, Wang X, Xu X, Su ZY, Cui Y, *et al*. Novel mutations in *CFAP44* and *CFAP43* cause multiple morphological abnormalities of the sperm flagella (MMAF). *Reprod Sci* 2019; 26: 26–34.
33 Martinez G, Kherraf ZE, Zouari R, Mustapha SF, Saut A, *et al*. Whole-exome sequencing identifies mutations in *FSIP2* as a recurrent cause of multiple morphological abnormalities of the sperm flagella. *Hum Reprod* 2018; 33: 1973–84.
34 Lorès P, Coutton C, El Khouri E, Stouvenel L, Givelet M, *et al*. Homozygous missense mutation L673P in adenylate kinase 7 (AK7) leads to primary male infertility and multiple morphological anomalies of the flagella but not to primary ciliary dyskinesia. *Hum Mol Genet* 2018; 27: 1196–211.
35 Coutton C, Martinez G, Kherraf ZE, Amiri-Yekta A, Boguenet M, *et al*. Bi-allelic mutations in *ARMC2* lead to severe astheno-teratozoospermia due to sperm flagellum malformations in humans and mice. *Am J Hum Genet* 2019; 104: 331–40.

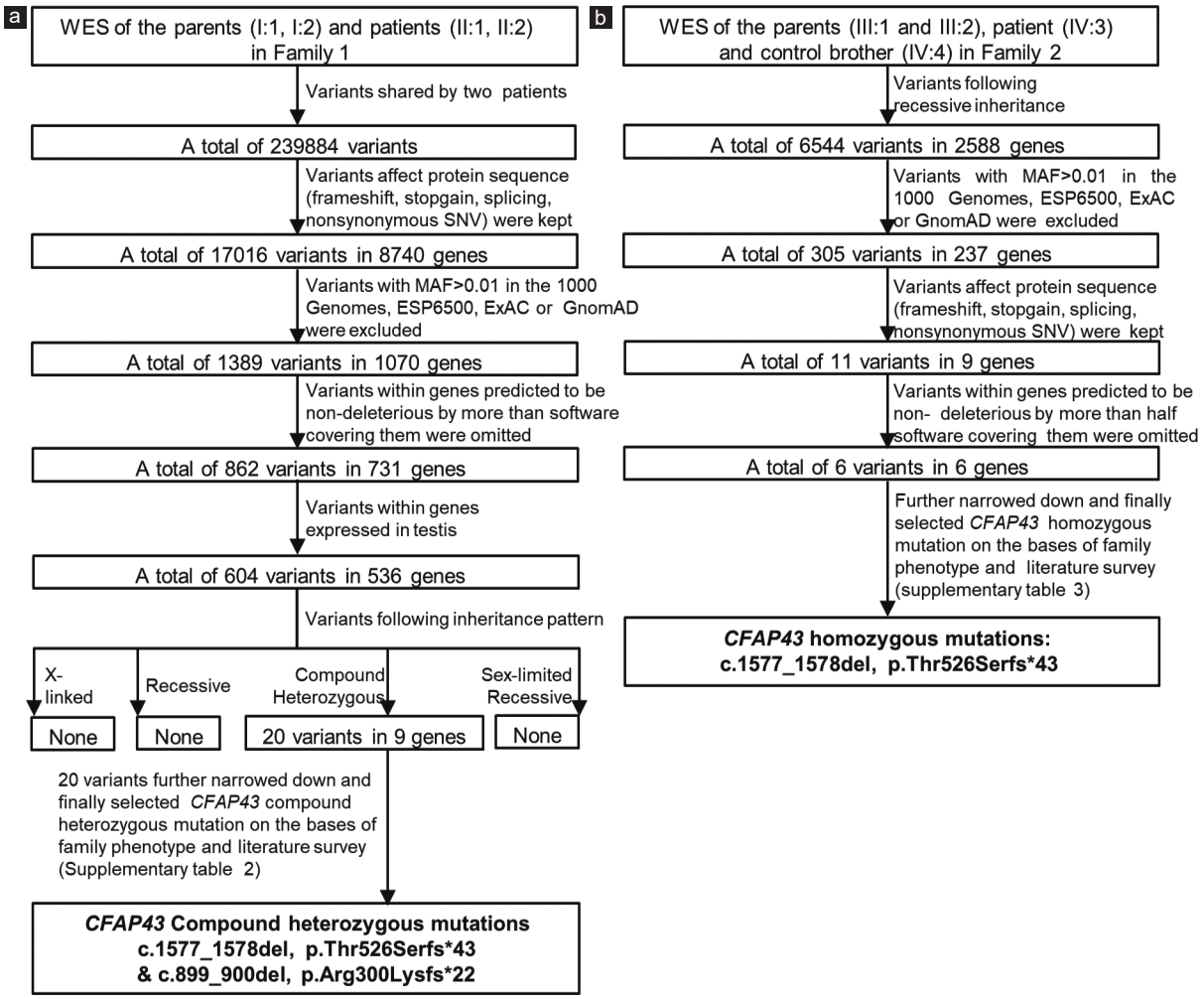

Supplementary Figure 1: Whole-exome sequencing (WES) analysis pipeline for (a) Family 1 and (b) Family 2.

Supplementary Table 1: Primers for polymerase chain reaction and Sanger sequencing of *CFAP43* variants

CFAP43 variants	*Product size (bp)*	*Forward primer*	*Reverse primer*
c.1577_1578del, p.Thr526Serfs*43	442	ATCAGGAGAATCCCTCATCC	TTACCTCTTCACATGCCAAG
c.899_900del, p.Arg300LysfsTer22	395	GCTCCTCTCTCTAATCTAGC	ATGTGACAGATCTGACATCC

Supplementary Table 2: Details of filtered variants from whole-exome sequencing analysis pipeline for family 1

Gene name	*Mutation type*	*cDNA change*	*Phenotypes of mutant mice from MGI or literature, or expression in testes*
ANKRD36C	Nonsynonymous SNV	C98T	Mutant mice have a mottled retina with photoreceptor degeneration and male infertility associated with oligozoospermia and asthenozoospermia
ANKRD36C	Frameshift substitution	1577_1579G	The same as above
CELA3B	Nonsynonymous SNV	G358A	The expression of this gene is not detectable in human testis
CELA3B	Frameshift substitution	2752_2753T	The same as above
CFAP43	Frameshift substitution	1577_1578G	Mice homozygous for a knock-out allele exhibit complete male sterility, asthenozoospermia, and teratozoospermia characterized by short, thick, and coiled flagella and sperm axonemal defects
CFAP43	Frameshift substitution	899_901A	The same as above
NBPF1	Nonsynonymous SNV	G1714A	Mice homozygous for a null allele exhibit partial (in utero or perinatal) lethality, hyperactivity, and increased vertical activity
NBPF1	Nonsynonymous SNV	T35G	Mice homozygous for a knock-out allele display delayed mammary tumor progression, impaired intestinal absorption of cholesterol, decreased gastric mucus accumulation, reduced secretion and accumulation of gallbladder mucin, and decreased susceptibility to cholesterol gallstone formation
PABPC3	Frameshift substitution	232_236T	Homozygotes for a null allele show high brain AEA levels, reduced pain sensation, altered behavioral responses to AEA, and sex-specific changes in ethanol intake and sensitivity. Homozygotes for the C385A variant show enhanced cued fear extinction and reduced anxiety-like behavior
PABPC3	Nonframeshift substitution		The same as above
PABPC3	Frameshift substitution	301_309G	Homozygotes for a null allele show high brain AEA levels, reduced pain sensation, altered behavioral responses to AEA, and sex-specific changes in ethanol intake and sensitivity. Homozygotes for the C385A variant show enhanced cued fear extinction and reduced anxiety-like behavior
PABPC3	Nonsynonymous SNV	C17T	The same as above
PIK3C2G	Frameshift substitution	595_596G	Homozygous null mice display hypoplasia of gut-associated lymph tissue due to defects in lymphocyte migration
PIK3C2G	Frameshift substitution	24_25T	The same as above
PRIM2	Frameshift substitution	899_901A	Mice homozygous for a null allele are viable and fertile with no gross abnormalities
PRIM2	Frameshift substitution	497_498A	The same as above
RRP12	Splicing	1657+3A>C	Homozygotes for targeted null mutations exhibit a 1 h shorter circadian period under constant darkness and reduced expression of another circadian gene in the suprachiasmatic nucleus in response to acute light exposure
RRP12	Nonsynonymous SNV	A1178T	The same as above
SPTA1	Splicing	565-3C>T	Mice homozygous or heterozygous for alleles of this gene exhibit varying degrees of hematopoietic defects
SPTA1	Frameshift substitution	51_52A	The same as above

MGI: mouse genome informatic; AEA: anandamide; SNV: single-nucleotide variant

Supplementary Table 3: Details of filtered variants from whole-exome sequencing analysis pipeline for family 2

Gene name	*Mutation type*	*cDNA change*	*Phenotypes of mutant mice from MGI or literature*
CFAP43	Frameshift	1577_1578G	Mice homozygous for a knock-out allele exhibit complete male sterility, asthenozoospermia, and teratozoospermia characterized by short, thick, and coiled flagella and sperm axonemal defects
MYO15A	Nonsynonymous SNV	C10393T	Mutations in this gene result in profound deafness and neurological behavior
KRTAP9-9	Nonsynonymous SNV	G422A	In the hair cortex, hair keratin intermediate filaments are embedded in an interfilamentous matrix, consisting of hair KRTAP, which are essential for the formation of a rigid and resistant hair shaft through their extensive disulfide bond cross-linking with abundant cysteine residues of hair keratins. The matrix proteins include the high-sulfur and high-glycine-tyrosine keratins
HTT	Nonsynonymous SNV	A107C	Null mutants gastrulate abnormally and die in utero. Conditional mutants are small with progressive neurodegeneration. Knock-ins of 20–150 CAG repeat units variably mimic Huntington's with late-onset motor defects, reactive gliosis, and neuronal inclusions
KRT25	Nonsynonymous	A716C	Mutations in this gene have a defect in hair formation resulting in a wavy coat and curly vibrissae
DONSON	Nonsynonymous	A752G	Homozygous knockout is early embryonic lethal. Heterozygous knockout causes no observable phenotype

MGI: mouse genome informatic; SNV: single-nucleotide variant; KRTAP: keratin-associated protein

Supplementary Table 4: Semen characteristics in the subjects carrying *CFAP43* mutations

Patient identified in the study	*cDNA change*	*Effect on protein, or protein alteration*	*Semen volume (ml)*	*Sperm count (10^6 ml)*	*Motility (%)*	*Immotile (%)*	*MMAF phenotype*	*Reference*
P003	c.2802T>A	p.Cys934*	2.2–3.8	16.1–39.4	0	100	Yes	2
P028	c.253C>T	p.Arg85Trp	1.5–2.5	16.1–39.4	2	98	Yes	
P029	c.386C>A	p.Ser129Tyr	2.5–4.0	12.2–18.9	1	99	Yes	32
P6	c.3661-2A>	NA	3.0	15.8	0	100	Yes	
P1	c.1140_1143del	p.Asn380Lysfs*3	2.3	7.6	0	100	Yes	11
P8	c.739A>T	p.Lys247*	2.4	25.8	0	100	Yes	
P9	c.1474G>C	p.Gln492Arg	3.5	32.1	0	100	Yes	
P10	c.4600C>G	p.Leu1534Val	4.1	19.2	0	100	Yes	
P5	c.4963C>T	p.Arg1655*	2.9	20.1	0	100	Yes	
P=10	c.3541–2A>C c.1240_1241delGT c.2658G>A c.2680C>T c.3882delA c.3352C>T c.1302dupT c.1040T>C c.2141+5G>A	p.Ser1181Lysfs*4 p.Val414LeufsTer46 p.Trp886Ter p.Arg894Ter p.Glu1294AspfsTer47 p.Arg1118Ter p.Leu435SerfsTer26 p.Val347Ala p.Lys714Val*11	3.5±1.4 (*n*=8)	27.2±23.4	0±0 (*n*=9)	100	Yes	10
P=2	c.899_900del c.1577_1578del	p.Arg300Lysfs*22 p.Thr526Serfs*43	3.3	07	0	100	Yes	Current study
P1	c.1577_1578del	p.Thr526Serfs*43	2–3	6–9	0	100	Yes	Current study

Supplementary Table 5: Percentages of involvement of the different sperm flagellum reported genes in the different cohorts

Gene	*Protein features*	*Percentage of involvement (%)*	*Reference*
DNAH1	Dynein heavy chain	28	7
CFAP65	Coiled-coil domain-containing protein	6.8	12
CFAP43 and CFAP44	WD repeat domains	7.5 22.22 30.8	2 32 11
FSIP2	AKAP4 interacting domain	5.1	33
AK7	ADK domain, coiled coil domain, DPY30 domain	1.2	34
WDR66 (CFAP251)	calcium regulating EF-hand domain	9	15
CFAP69	Armadillo-type α-helical repeats	2.6	18
ARMC2	Armadillo repeat-containing protein 2	2.4	35